Pre-metric SO(2) Connections, Quadratic Embeddings, and Angular Monodromy: Optical Origin, Holonomy, and Lensing Signatures

Bernard Lavenda
Independent Researcher, Shoresh, Israel. E-mail: bhlavenda@gmail.com

We develop a pre-metric framework for an SO(2) connection on a principal S^1-bundle over a two-dimensional base. The connection is derived from the logarithmic derivative of a refractive index via the Gauss-Log-Index projection principle, giving a direct optical interpretation. The construction admits a reciprocal symmetry $n \leftrightarrow 1/n$, producing a dual optical sector with no intrinsic cap on the speed of light; propagation is governed by the connection, not by a fixed causal cone or null geodesics. Using the Hodge decomposition on the base, we separate the connection into exact (spin-0), co-exact (spin-1 curvature), and harmonic (topological monodromy) components [1]. The quadratic embedding $(d\theta + A)^2$ of the connection into a total metric is proved non-invertible: the antisymmetric curvature dA (spin-1) cannot be recovered from the symmetric metric block. This explains why metric (spin-2) observations alone are blind to spin-1 holonomy [2, 3].

When the connection is not integrable ($F = dg \neq 0$), the angular fibre acquires curvature, producing a measurable SO(2) holonomy. In gravitational lensing, this holonomy manifests as a centroid separation between lensing and dynamical channels — a single-signed, monotonic signature that cannot be reproduced by shear or flexion alone. We provide numerical illustrations on a uniform parameter grid. The transition from the Abelian SO(2) regime to a non-Abelian SO(3) regime is characterised by the failure of the fibre embedding's normality condition, leading to quadratic connection terms in the curvature. The analogy with Dirac/Klein-Gordon squaring is drawn: squaring a connection loses spin-1 information, just as squaring a Dirac spinor loses fermionic degrees of freedom.

The Aharonov-Bohm (AB) effect is shown to be a classical optical holonomy — a spin-1 effect — unifying gravitational lensing and electromagnetic phase shifts as manifestations of connection holonomy. Both effects are described by an effective refractive index; the minimal charge coupling $q \oint A_\mu dx^\mu$ is a subcategory of this optical description. The phase is independent of $\hbar$, reflecting its purely classical/geometric origin. The complex phase is replaced by a real rotation. This interpretation completely undercuts the anyon narrative (Wilczek, 1982 [4, 5]), which misinterprets the AB effect as a quantum statistical phenomenon. As shown in Lavenda and Dunning-Davies (1989 [6]), no probability distribution exists between the binomial (fermionic) and negative binomial (bosonic) distributions, rendering intermediate statistics stillborn.

1 Introduction

General relativity (GR) is a metric theory of gravity: the fundamental object is the metric, and the Levi-Civita connection is derived from it. The Einstein equations contract the Riemann tensor to the Einstein tensor, mixing sectional curvatures of different orthogonal 2-planes [7]. The Ricci tensor contains both trace (spin-0) and traceless symmetric (spin-2) parts, while the Weyl tensor (also spin-2) is not determined locally by matter. The result is that the Einstein tensor does not cleanly separate the spin-0, spin-1 and spin-2 channels of gravity. In linearised GR, the propagating field is the metric perturbation; its transverse-traceless decomposition artificially isolates a spin-2 component, but this separation is gauge-dependent and does not arise from an intrinsic geometric splitting.

This paper takes a different path. We develop a pre-metric framework in which the fundamental object is an independent SO(2) connection g on a principal S^1-bundle over a two-dimensional base. No metric is required to define the connection or its curvature $F = dg$. The Hodge decomposition on the base separates the connection into exact (spin-0), coexact (spin-1 curvature) and harmonic (topological monodromy) components. This separation is intrinsic: the connection itself carries spin-1, its curvature is a scalar (spin-0), and a quadratic tidal term $(g_t - g_r)^2$ emerges as a symmetric traceless (spin-2) object from the quadratic embedding of the connection into a total metric.

The central claims are:

- The SO(2) connection g is a genuine pre-metric geometric field whose curvature $F = dg$ measures Faraday obstruction (spin-0), whose components define a spin-1 vector, and whose quadratic tidal term gives a spin-2 effect.
- The quadratic embedding $(d\theta + g)^2$ into a total metric is not invertible: the antisymmetric curvature dg (spin-1) cannot be recovered from the symmetric metric block.

- The Hodge decomposition yields a topological monodromy (real AB rotation) independent of local curvature.
- A non-integrable connection ($F \neq 0$) produces SO(2) holonomy, a centroid separation in gravitational lensing, and other spin-1 observables that cannot be reproduced by any metric theory.
- The AB effect is a classical optical holonomy — a spin-1 effect that is neither electrodynamic nor quantum in origin. It provides the fundamental experimental validation of the pre-metric framework, demonstrating that connection holonomy has observable physical consequences independent of any metric. This geometric interpretation definitively refutes the anyon narrative (Wilczek, 1982 [4, 5]), which misinterprets the AB effect as a quantum statistical phenomenon. As shown in Lavenda and Dunning-Davies (1989 [6]), no probability distribution exists between the binomial (fermionic) and negative binomial (bosonic) distributions, rendering intermediate statistics unphysical.

The paper is organised as follows. §2 introduces the pre-metric SO(2) connection, the angular line element, and the Hodge decomposition. §3 defines the curvature, divergence and mixed obstruction. §4 proves the non-invertibility of the quadratic embedding and discusses the structural isomorphism with ADM and Kaluza-Klein. §5 interprets holonomy and monodromy, including the AB analogy, and explicitly demonstrates its optical/geometric nature while refuting the anyon interpretation. §6 describes the transition to the non-Abelian regime in full detail, including the normality condition, the breakdown to SO(3), and the toy model yielding quadratic commutator terms. §7 separates the spin channels and includes a dedicated subsection on the algebraic versus curvature-derived origin of the spin-2 tidal term. §8 presents the optical derivation of the connection via the Gauss-Log-Index projection principle, with the reciprocal symmetry $n \leftrightarrow 1/n$. §9 describes the spin-1 lensing signature and centroid separation, with a consistent numerical illustration. §10 compares interferometric diagnostics (Michelson vs. Sagnac). §11 draws the analogy with Dirac/Klein-Gordon and Hamiltonian/Lagrangian information loss. §12 discusses fictitious vs. real forces and provides a pointed critique of why metric theories (GR, TeVeS) and MOND cannot produce the spin-1 centroid effect. §13 compares the curvature decomposition and Weyl tensor in metric gravity versus the pre-metric framework. §14 examines how far one can go with the connection alone. §15 concludes.

2 Pre-metric SO(2) connection

2.1 Geometric setting

Let (M^2, η_{ab}) be a two-dimensional manifold (Lorentzian or Riemannian as context requires) with local coordinates $x^a = (t, r)$ and a background metric η_{ab}. Consider a principal S^1-bundle

$$S^1 \hookrightarrow P \to M^2 \,,$$

with fibre coordinate $\theta \in [0, 2\pi)$. Since $\mathrm{SO}(2) \cong S^1$ is Abelian, a connection on P is specified by a single real one-form on the base [2].

The angular connection is a one-form

$$g = g_a dx^a = g_t dt + g_r dr \in \Omega^1(M^2) \,. \tag{1}$$

The angular line element on the total space may be written formally as

$$ds_{\mathrm{ang}} = g \wedge d\theta \,, \tag{2}$$

or, when g is a scalar function, as $ds_{\mathrm{ang}} = g\, d\theta$. The connection g and its exterior derivative dg are defined without reference to any metric on M^2; a background metric is used only to raise indices or form divergences.

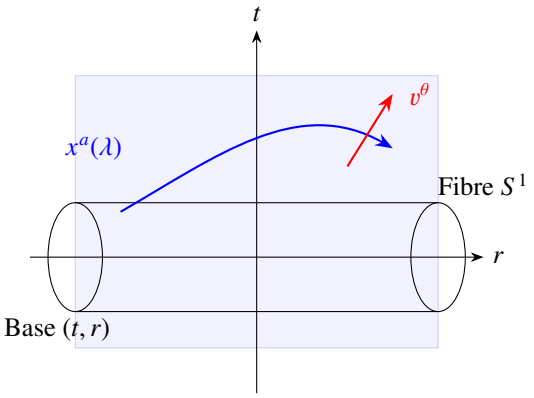

Fig. 1: The angular bundle as a cylinder. The base is the (t, r) plane; the fibre is S^1. A base trajectory (blue) and a vertical lift (red) are shown.

2.2 Hodge decomposition on two-manifolds

Let M^2 be oriented and equipped with a Riemannian metric for Hodge theory. The Hodge decomposition for one-forms on a compact oriented two-manifold (or on $\mathbb{R}^2$ with suitable decay) is [8]

$$g = d\phi + \star d\psi + \omega_{\mathrm{harm}} \,, \tag{3}$$

where ϕ, ψ are scalar potentials, $\star$ is the Hodge star, and ω_{harm} is harmonic: $d\omega_{\mathrm{harm}} = 0$, $\delta\omega_{\mathrm{harm}} = 0$. On simply connected domains $\omega_{\mathrm{harm}} = 0$; on domains with nontrivial first cohomology $H^1(M^2) \neq 0$ there exist closed one-forms that are not exact [7], and ω_{harm} may be nonzero representing global monodromy.

Separation of curvature and source. Write g as in (3). Then:

1. The curvature $F = dg$ depends only on the co-exact part: $F = d(\star d\psi)$;
2. The divergence $J = \delta g$ depends only on the exact part: $J = \delta d\phi = \Delta\phi$, the Laplace-Beltrami operator;

3. The harmonic term ω_{harm} carries global holonomy and is invisible to both F and J.

2.3 Explicit forms in Cartesian and polar coordinates

On the punctured plane $\mathbb{R}^2\backslash\{0\}$

$$d\theta = \frac{-y\,dx + x\,dy}{x^2 + y^2}\,, \tag{4}$$

which is closed but not exact, generating $H^1(\mathbb{R}^2\backslash\{0\}) \cong \mathbb{R}$, with $\oint_{S^1} d\theta = 2\pi$.

3 Curvature, divergence, and mixed obstruction

The curvature two-form is

$$F = dg = (\partial_t g_r - \partial_r g_t)\, dt \wedge dr\,, \tag{5}$$

a scalar multiple of the area form. The divergence is

$$J = \nabla_a g^a = -\partial_t g_t + \partial_r g_r\,, \tag{6}$$

when indices are raised with a background metric.

The angular two-form $ds_{\text{ang}} = g \wedge d\theta$ has exterior derivative

$$d(ds_{\text{ang}}) = dg \wedge d\theta\,. \tag{7}$$

This mixed obstruction vanishes if either $dg = 0$ (integrable connection) or $d\theta$ is exact (no angular monodromy). When both are nonzero, it quantifies the coupling between base curvature and topological angular non-integrability.

4 Quadratic embedding and structural isomorphism

4.1 Universal squared structure

A common algebraic pattern appears in several geometric frameworks: a total-space metric contains a squared term

$$ds^2_{\text{total}} = ds^2_{\text{base}} + \Phi\,(d\varphi + A)^2\,, \tag{8}$$

where φ denotes a generic fibre coordinate (e.g., the S^1 angle θ in our specific case, or a Kaluza-Klein coordinate), and A is a one-form on the base. Instances include the angular bundle ($\varphi = \theta$, $A = g$), ADM decomposition (shift vector) [8], and Kaluza-Klein reduction (A as gauge potential) [9]. Expanding the square produces off-diagonal cross terms and a symmetric quadratic contribution $A_a A_b\, dx^a dx^b$. The antisymmetric derivative information dA (field strength) is not present in the symmetric quadratic term alone.

4.2 Non-invertibility of the quadratic embedding

The map $A \mapsto g_{\text{total}}$ is quadratic and not injective: distinct one-forms A can produce the same symmetric metric block. Consequently, the antisymmetric curvature dA (spin-1) cannot be recovered from the metric block alone. This is the spin-1 erasure by quadratic embedding [8].

4.3 Structural isomorphism across frameworks

The algebraic form (8) appears in the angular connection, in the ADM shift [8], and in Kaluza-Klein constructions [9]. The difference among these contexts lies in the additional structural constraints: KK typically imposes a cylinder condition that promotes the fibre translation to a gauge symmetry; ADM treats the shift as a coordinate freedom (Lagrange multiplier); the angular bundle treats g as a genuine connection on a principal S^1-bundle. The isomorphism is algebraic; the geometric interpretation depends on the global structure and constraints.

5 Classical interpretation: holonomy, monodromy, precession, and the optical nature of the AB effect

5.1 Holonomy and parallel transport

Parallel transport in the S^1 fibre along a curve γ with tangent $\dot\gamma$ is governed by the pullback of g [2]:

$$\frac{d\theta}{d\lambda} + g(\dot\gamma(\lambda)) = 0\,,$$

where θ is the fibre angle. For a closed curve γ bounding a surface Σ

$$\Delta\theta = -\oint_\gamma g = -\int_\Sigma dg = -\int_\Sigma F\,, \tag{9}$$

so curvature produces holonomy via Stokes' theorem.

5.2 Holonomy vs. monodromy: local curvature vs. global topology

It is essential to distinguish between two distinct geometric phenomena: holonomy arising from local curvature, and monodromy arising from global topology.

1. **Holonomy** is the net change of a fibre quantity (e.g., an angle or a vector) when it is parallel transported around a contractible closed curve γ. By Stokes' theorem, the holonomy equals the flux of the curvature $F = dg$ through any surface Σ bounded by γ:

   $$\Delta\theta_{\text{hol}} = -\oint_\gamma g = -\int_\Sigma dg = -\int_\Sigma F\,.$$

   Thus holonomy vanishes if $F = 0$ locally (flat connection) and the loop is contractible. Holonomy is a local effect: it depends on the curvature field inside the loop.

2. **Monodromy** arises when the base manifold is not simply-connected, e.g., the punctured plane $\mathbb{R}^2\backslash\{0\}$. A closed curve γ that winds around the puncture cannot be contracted to a point without crossing the puncture. Even if the connection is flat ($F = 0$) everywhere, parallel transport around a non-contractible loop can produce a non-zero rotation. This is a topological effect,

independent of any local curvature. For the canonical angular one-form $d\theta$ on the punctured plane,

$$\oint_{S^1} d\theta = 2\pi \neq 0\,,$$

even though $d(d\theta) = 0$. This monodromy is encoded in the harmonic component ω_{harm} of the Hodge decomposition (3).

5.3 The AB effect and gravitational lensing: two sides of the same coin

5.3.1 The optical analogy

The AB effect and gravitational lensing are both classical optical holonomies. In both cases, a connection determines the phase shift, not the field strength. The phase shift is described by an **effective refractive index** for the probe.

In gravitational lensing, a photon traverses a gravitational field, which acts as a medium with an effective refractive index. For a Schwarzschild lens, the refractive index is

$$n(r) \approx 1 + \frac{GM}{c^2 r}\,,$$

where r is the impact parameter. The phase shift acquired over a path length ℓ through this effective medium is

$$\Delta\theta \approx \frac{2\pi}{\lambda}\int (n-1)\,d\ell \approx \frac{2\pi}{\lambda}\,\frac{GM}{c^2 r}\,\ell\,.$$

In the AB effect, the electron traverses a region with an effective refractive index:

$$n_{\text{eff}} = 1 - \frac{qA}{p}\,,$$

where p is the electron's momentum. The phase shift is then:

$$\Delta\theta = \frac{2\pi}{\lambda}\int (n_{\text{eff}} - 1)\,d\ell = \frac{q}{p}\oint A_\mu\,dx^\mu\,.$$

The factor q/p is a geometric constant (the inverse of the de Broglie wavelength) and $\hbar$ does not appear. The AB phase is a purely classical/optical effect. The minimal charge coupling $q/\hbar \oint A_\mu\,dx^\mu$ is a subcategory of this more general optical description, applicable when one chooses to express the phase in terms of the quantum mechanical wavefunction. But the holonomy itself is independent of $\hbar$.

Both effects are geometric/optical: see the Table at the top of the next page.

5.3.2 Interference reveals holonomy

The key point is this: the AB effect and gravitational lensing are measured in exactly the same way — through interference.

The AB effect is measured using electron interference. The relative phase shift between two electron paths around a solenoid produces a shift in the interference pattern. Gravitational phase shifts are measured using photon interference (e.g., the Shapiro delay, gravitational lensing, or interferometric measurements of the phase shift due to a gravitational potential).

In both cases, the interference pattern reveals the holonomy of a connection. The fact that one probe is an electron (fermion, spin-1/2) and the other is a photon (boson, spin-1) is **irrelevant** to the effect itself. Both probes are quantum mechanical, but the phase they measure is a **classical geometric holonomy**.

The only reason the AB effect is often called "quantum" is historical: it was discovered in the context of quantum mechanics (electron interference), while gravitational lensing was discovered in the context of classical optics (light bending). But the underlying geometry is the same.

5.3.3 The AB effect is SO(2), not U(1)

An essential clarification must be made: the AB effect is fundamentally an **SO(2)** phenomenon, not a U(1) phenomenon.

The U(1) representation (complex phase $e^{i\phi}$) is how a charged quantum probe (an electron, a pion, any charged particle) experiences the holonomy of the electromagnetic connection A_μ. The factor $q/\hbar$ is a conversion factor that depends on the probe's charge and the units of measurement. Photons, being neutral, do not couple to A_μ via minimal coupling; they experience geometric phases through the refractive index of the medium — exactly as described in the optical analogy above.

The holonomy itself, however, is a real rotation of a two-vector:

$$\begin{pmatrix} v_x \\ v_y \end{pmatrix} \longrightarrow \begin{pmatrix} \cos\theta & -\sin\theta \\ \sin\theta & \cos\theta \end{pmatrix}\begin{pmatrix} v_x \\ v_y \end{pmatrix}. \tag{10}$$

This is exactly the SO(2) holonomy of the pre-metric framework (see §7.1 for the representation theory). The AB phase, $\psi \to e^{i\phi}\psi$, is replaced by the real rotation of the two component vector, (10).

Similarly, in gravitational lensing, the image basis undergoes an SO(2) rotation, producing the centroid separation (§9). Both effects are:

- **SO(2) holonomies** of a connection.
- **Classical geometric effects**, independent of the spin-statistics of the probe.
- **Real rotations**, not complex phases of a wavefunction.

The anyon narrative (Wilczek, 1982 [4, 5]) misinterprets the U(1) representation as a quantum statistical phase. But the underlying geometry is SO(2) — a real rotation — which has nothing to do with fermionic exchange statistics. The AB effect is a classical optical holonomy, not a quantum statistical phenomenon.

Effect	Probe	Phase Shift	Connection
Gravitational lensing	Photon (spin-1)	$\Delta\theta = \frac{2\pi}{\lambda}\frac{GM}{c^2 r}\,\ell$	$\omega = -\frac{n'r+n}{n}\,d\theta$ (§8)
Aharonov-Bohm	Electron (spin-1/2)	$\Delta\theta = \frac{q}{p}\oint A_\mu\,dx^\mu$	Electromagnetic A_μ

5.3.4 Reciprocal symmetry $n \leftrightarrow 1/n$

As we shall show in §8.1, the pre-metric connection admits a reciprocal symmetry:

$$n \leftrightarrow \frac{1}{n} \quad \Longrightarrow \quad A(r) \longrightarrow -A(r)\,.$$

For gravitational lensing, replacing n by $1/n$ changes the sign of the phase shift: $\Delta\theta \to -\Delta\theta$.

In the AB effect, this corresponds to reversing the direction of the solenoid's current, which changes the sign of the vector potential: $A_\mu \to -A_\mu$. This symmetry proves that the AB phase is governed by the same geometric reciprocity as optical gravitational lensing. It is an optical/geometric effect, not a quantum statistical one.

5.3.5 Conclusion

The AB effect and gravitational lensing are identical in nature: both are classical optical holonomies revealed through interference. The only difference is the probe used to measure them — electrons for the AB effect, photons for gravitational lensing. Both probes are quantum mechanical, but the effect they measure is a classical geometric holonomy. The AB effect is not a quantum statistical phenomenon; it is a spin-1 holonomy of an SO(2) connection, exactly as described by the pre-metric framework.

6 Transition to the non-Abelian regime

6.1 Normality condition

Let $\iota : M^2 \hookrightarrow M^{n+1}$ be an isometric embedding with unit normal(s) along the fibre. The normality condition requires that the second fundamental form K_{ab} have no components tangential to the base [10]:

$$K_{ab}\,T^a = 0 \quad \text{for all } \; T^a \in TM^2\,.$$

6.2 Breakdown: SO(2) to SO(3)

When the normality condition fails, the fibre may thicken from S^1 to a portion of S^2.

The relevant structure group is SO(3), but the fibre itself is the homogeneous space $S^2 \cong \mathrm{SO}(3)/\mathrm{SO}(2)$. The connection is no longer independent; it is absorbed into the metric via the quadratic embedding $(d\theta + A)^2$.

In the Abelian SO(2) case the curvature 2-form is $\Omega = d\omega$ (no $\omega \wedge \omega$ term because the Lie algebra is one-dimensional and the wedge product of two 1-forms is symmetric). When the structure group is enlarged to SO(3), the Cartan structure equations become non-Abelian:

$$\Omega^I = d\omega^I + \frac{1}{2}\,C^I_{JK}\,\omega^J \wedge \omega^K, \tag{11}$$

with structure constants C^I_{JK} of $\mathfrak{so}(3)$. The quadratic term $\omega \wedge \omega$ is the hallmark of a Yang-Mills theory. However, in the present geometric setting, this non-Abelian connection is not an independent field; it is derived from the metric on the total space. The transition from the Abelian SO(2) regime to the non-Abelian regime therefore represents a geometric phase transition where the fibre S^1 "inflates" to S^2 and the connection is subsumed into the metric.

6.2.1 Toy model for the non-Abelian transition

To illustrate how the quadratic commutator term $\omega \wedge \omega$ appears when the fibre thickens to S^2, consider a three-dimensional total space with coordinates (r, Θ, Φ) and a metric

$$ds^2 = dr^2 + G^2(r)\left(d\Theta^2 + \sin^2\Theta\,d\Phi^2\right),$$

where $G(r)$ is a warp factor. The isometry group of the fibre S^2 is SO(3). Take an orthonormal coframe

$$e^1 = dr, \quad e^2 = G\,d\Theta, \quad e^3 = G\sin\Theta\,d\Phi\,.$$

Cartan's first structure equations $de^i + \omega^i_j \wedge e^j = 0$ yield the non-zero connection 1-forms:

$$\omega^2_3 = \cos\Theta\,d\Phi\,, \qquad \omega^2_1 = \frac{G'}{G}\,e^2\,, \qquad \omega^3_1 = \frac{G'}{G}\,e^3\,.$$

The curvature 2-forms are

$$\Omega^2_3 = d\omega^2_3 + \omega^2_1 \wedge \omega^1_3 + \omega^3_1 \wedge \omega^3_2\,,$$

and the explicit computation gives

$$\Omega^2_3 = \left(1 - (G')^2\right)e^2 \wedge e^3\,,$$

$$\Omega^2_1 = -\frac{G''}{G}\,e^1 \wedge e^2, \qquad \Omega^3_1 = -\frac{G''}{G}\,e^1 \wedge e^3.$$

The quadratic term $\omega \wedge \omega$ contributes to the curvature because the structure group is non-Abelian. The 2D-planes need to be oriented into the higher dimensions; these terms provide "sources" of curvature, rather than curvature themselves. In the Abelian SO(2) limit, the fibre is a circle and the corresponding connection would have no $\omega \wedge \omega$ term. This explicit geometry shows that when the fibre is a sphere, the quadratic commutator terms naturally arise [11].

Component	Expression	Spin	Geometric meaning
Divergence	$J = \nabla^a g_a$	0	scalar source (Ampère)
Curvature	$F = dg$	0 (scalar)	Faraday flux, holonomy
Connection itself	g	1	vector potential, twist
Tidal term	$(g_t - g_r)^2$	2	traceless symmetric, shear

Table 1: Spin decomposition of the SO(2) connection on a 2-D base.

6.3 Origin of the spin-2 tidal term

The decomposition of a one-form g on a two-dimensional base into irreducible components under SO(2) yields a scalar divergence $J = \nabla^a g_a$ (spin-0), a scalar curvature $F = dg$ (spin-0 as a 2-form, but the connection itself carries spin-1), and a symmetric traceless combination $(g_t - g_r)^2$ (spin-2).The latter is not a curvature; it is an algebraic quadratic invariant. Its interpretation as a spin-2 tidal deformation follows from the quadratic embedding of the connection into a total metric (§4). When the coframe $e^\theta = Gd\theta + g_a\, dx^a$ is squared, the symmetric part of the base metric receives a contribution $g_a g_b\, dx^a dx^b$. In an orthonormal frame, the traceless part of the 2×2 matrix $g_a g_b$ is exactly $\frac{1}{2}(g_t - g_r)^2$ (up to a factor). This term is absent when the connection is umbilic, i.e., when $g_t = g_r$. Hence the deviation from umbilicity directly sources a spin-2 component in the metric shadow. In gravitational lensing, this term produces a shear-like distortion that is orthogonal to the standard metric shear.

7 Metric squaring, spin channels, and the SO(2) limit

The pre-metric formulation separates the angular connection into three irreducible components. The connection g itself is a one-form; in two dimensions its components transform as a vector under rotations — this is the spin-1 channel. Its curvature $F = dg$ is a 2-form, which in 2D is dual to a scalar (spin-0). The quadratic tidal term $(g_t - g_r)^2$ is a symmetric traceless object (spin-2). Table 1 summarises the decomposition.

The quadratic embedding $(d\theta + g)^2$ into a total metric retains only spin-0 and spin-2 components; the spin-1 channel is lost.

7.1 Spin-2 in the pre-metric framework: algebraic vs. curvature-derived

In a two-dimensional base manifold, the Riemann tensor has only one independent component:

$$R_{abcd} = \frac{R}{2}\,(g_{ac}\, g_{bd} - g_{ad}\, g_{bc})\,,$$

where R is the Ricci scalar. There is no Weyl tensor and no propagating spin-2 degree of freedom. Therefore, any "spin-2" object appearing in the pre-metric framework cannot arise from curvature; it must come from a different geometric operation.

The pre-metric SO(2) connection $g = g_a dx^a$ is a one-form whose components transform as a vector under the rotation group of the base. The connection coefficients g_a act like the second fundamental form K_{ab} of the fibre embedding. Under an SO(2) rotation by angle θ

$$\begin{pmatrix} g_t \\ g_r \end{pmatrix} \longrightarrow \begin{pmatrix} \cos\theta & -\sin\theta \\ \sin\theta & \cos\theta \end{pmatrix} \begin{pmatrix} g_t \\ g_r \end{pmatrix}.$$

The deviation from umbilicity $(g_t - g_r)^2$ is the traceless part of the extrinsic curvature — the "shear" of the embedding. The spin-2 tidal term is the symmetric traceless product of the connection components:

$$Q = \begin{pmatrix} g_t^2 - g_r^2 & 2\, g_t\, g_r \\ 2\, g_t\, g_r & g_r^2 - g_t^2 \end{pmatrix}. \tag{12}$$

The magnitude of this spin-2 object is proportional to $(g_t^2 + g_r^2)$, and its orientation is determined by the ratio g_t/g_r. For a purely radial configuration ($g_t = 0$), the tidal term reduces to $(g_t - g_r)^2 = g_r^2$. This is not a curvature invariant; it is an algebraic quadratic invariant of the connection.

In the Gauss-Codazzi decomposition, the spin-0 quantity (6) is the trace, or mean curvature; the spin-1 quantity (5) is the normal, or Gauss curvature of the fibre; and the spin-2 quantity (12) is the traceless part of the extrinsic curvature, measuring the deviation from umbilicity.

In contrast, the spin-2 of metric theories (GR) is a gauge-dependent construct: it emerges only after imposing transverse-traceless gauge conditions on the metric perturbation, which artificially isolates a spin-2 component from the metric. This identification does not arise from an invariant decomposition of the Riemann tensor. In the pre-metric framework, no such gauge fixing is needed: the spin-2 tidal term is an intrinsic algebraic invariant of the connection, independent of any gauge choice.

In the pre-metric framework, the connection components g_t, g_r can propagate (e.g., satisfy wave equations derived from an action). The quadratic tidal term $(g_t - g_r)^2$ is an algebraic combination of these components; it does not possess independent dynamics of its own. It is not a propagating wave mode but a measure of the deviation from umbilicity. It becomes observable when the connection is squared to form a metric (quadratic embedding) or when the deviation from umbilicity influences lensing (the centroid separation).

Profile	$n(r)$	Domain	$A(r) = -(n'r + n)/n$
Eaton (retroreflector)	$\sqrt{1/r - 1}$	$0 < r < 1$	$1 - 1/[2(1 - r)]$
Schwarzschild (optical)	$(1 - 1/r)^{-1/2}$	$r > 1$	$(3 - 2r)/[2(r - 1)]$
Luneburg lens	$\sqrt{2 - r^2}$	$0 \leqslant r \leqslant 1$	$-2(1 - r^2)/r^2$
Maxwell fish-eye	$2/(1 + r^2)$	$r \geqslant 0$	$(1 + r^2)/(1 - r^2)$
Poincaré disk	$2/(1 - r^2)$	$0 \leqslant r < 1$	$-(1 + r^2)/(1 - r^2)$

Table 2: Canonical index profiles and their Cartan radial generators $A(r)$ from (13).

8 Optical origin: Gauss-Log-Index projection and dual representation

The angular connection on the base admits a direct optical interpretation: a refractive index $n(r)$ supplies an optical coframe whose volume form and Hodge duality define the Helmholtz decomposition. The optical metric is a convenient conformal representative, but it is not required for the connection or its curvature.

The conformal optical metric

$$ds^2 = n^2(r)\left(dr^2 + r^2 d\theta^2\right),$$

has the orthonormal coframe

$$e_1 = n(r)\, dr, \qquad e_2 = n(r)\, r d\theta\,.$$

Cartan's first structure equation $de^2 = \omega \wedge e^1$ gives

$$\omega = -\frac{n'r + n}{n}\, d\theta \equiv A(r)\, d\theta\,. \tag{13}$$

The Gauss-Log-Index projection principle is the statement that, when ω is a function of n alone and symmetric under $n \leftrightarrow 1/n$, the simplest such expression is the odd Joukowski combination

$$g = \omega = \frac{1}{2}\left(n - \frac{1}{n}\right) d\theta\,.$$

This projection is a normalisation convention; the geometric connection itself is given by (13) and is independent of that choice.

8.1 Reciprocal symmetry and the dual optical sector

The coframe construction admits a reciprocal symmetry $n \mapsto 1/n$. Replacing n by $1/n$ rescales the coframe conformally and modifies the radial generator of the connection:

$$A(r) \to A_{\,\mathrm{dual}}(r) = -A(r)\,.$$

This reciprocal operation produces the dual optical sector. The symmetry shows that the restriction $n \geqslant 1$ is a material, not a geometric, constraint. There is no intrinsic cap on the speed of light; propagation is governed by the connection, not by a fixed causal cone or null geodesics. In particular, the Hodge star and the associated Hodge Laplacian used in the Hodge decomposition (3) are defined by the coframe $e^a = n(r)\,\hat{e}^a$ and the induced volume form; they do not require a background Riemannian or Lorentzian metric on the base. The Lorentzian signature plays no structural role in the existence of the SO(2) connection or in the spin decomposition.

8.2 Representative examples

Table 2 displays explicit refractive-index profiles $n(r)$, their domains, and the corresponding radial generators $A(r)$.

These cases show that qualitatively distinct ray dynamics (bound, unbound, focusing, closed geodesics) arise from different choices of $n(r)$, while the pre-metric connection $\omega = A(r)\, d\theta$ and its curvature $F = d\omega$ remain the primary geometric objects [12, 13].

9 Spin-1 lensing signature and centroid separation

9.1 Pre-metric structure for lensing

The angular connection acts on the SO(2) fibre through the Lie-algebra generator ϵ^b_ϕ, so that the connection coefficients take the form

$$\Gamma^b_{\phi a} = g_a(t, r)\, \epsilon^b_\phi\,.$$

The curvature is obtained from the commutator of covariant derivatives,

$$R^\phi_{\theta rt} = \partial_t \Gamma^\phi_{\theta r} - \partial_r \Gamma^\phi_{\theta t}\,,$$

and substituting the form of the connection yields

$$R^\phi_{\theta rt} = (\partial_t g_r - \partial_r g_t)\, \epsilon^b_\phi = F\, \epsilon^b_\phi\,.$$

Thus the scalar Faraday obstruction $F = dg$ is precisely the coefficient of the infinitesimal SO(2) rotation on the fibre. This curvature is not the Riemann tensor of a metric theory; it is a pure $\mathfrak{so}(2)$ holonomy on the angular fibre.

The connection acts on an associated $\mathbb{R}^2$ bundle (the image plane). Parallel transport of a fibre vector v_i along a base trajectory $x^a(\lambda)$ obeys

$$\frac{dv_i}{d\lambda} = \Omega(\lambda)\, \epsilon_{ij} v_j\,, \qquad \Omega = g_a\, \dot{x}^a\,.$$

When the scalar Faraday obstruction $F = 0$, the rotation depends only on endpoints; when $F \neq 0$, closed loops accumulate a net rotation proportional to $\int F$.

9.2 Centroid separation

The rotation of the angular basis produces three observables: image twist, shear-like distortions, and a centroid separation between the lensing centroid (using the full connection) and the dynamical centroid (using the integrable part). The centroid offset is single-signed, monotonic, and cannot be reproduced by metric shear or flexion.

Combining the two components into $w = v_x + iv_y$, the transport equation becomes

$$\frac{dw}{d\lambda} = i\Omega w\,.$$

9.3 Numerical illustration

We now present a concrete, numerically tractable example that respects the pre-metric structure: the angular connection is a one-form on the base (t, r) with no $d\theta$ component. For simplicity we restrict to purely radial base trajectories and take the connection to be radial only:

$$g = g_r(r)\,dr\,, \qquad g_t = 0\,.$$

The Faraday obstruction (curvature) becomes

$$F = dg = \frac{dg_r}{dr}\,dr \wedge dt\,,$$

which is non-zero whenever g_r is not constant. This directly produces SO(2) holonomy.

Parallel transport. Along a radial trajectory $r(\lambda)$ with λ an affine parameter, the instantaneous rotation rate is

$$\Omega(\lambda) = g_r\big(r(\lambda)\big)\,\dot{r}(\lambda)\,,$$

where $\dot{r} = dr/d\lambda$. The complex basis $w = v_\theta + iv_\phi$ evolves as

$$\frac{dw}{d\lambda} = i\Omega(\lambda)w\,.$$

Choice of profile. A physically motivated profile is the derivative of a logarithmic potential:

$$g_r(r) = \tilde{\rho}_0\,\frac{d}{dr}\ln\Big((r-r_0)^2 + a^2\Big)^{-1/2} = -\tilde{\rho}_0\,\frac{r-r_0}{(r-r_0)^2+a^2}\,,$$

which is a Lorentzian (Cauchy) function centred at r_0 with width a. This profile arises naturally from the Gauss-Log-Index projection principle (§8) when the refractive index is chosen as

$$n(r) = \exp\left(-\tilde{\rho}_0 \arctan\left(\frac{r-r_0}{a}\right)\right).$$

The amplitude $\tilde{\rho}_0$ controls the integrated curvature, and the offset x_0 (here r_0) shifts the region of non-integrability.

We use this radial connection with the Lorentzian profile:

$$g_r(r) = -\tilde{\rho}_0\,\frac{r-r_0}{(r-r_0)^2+a^2}\,,$$

where $a = 1$ in the numerical example. For a radial line of sight $r(\lambda) = \lambda$ ($\dot{r} = 1$), the rotation angle is

$$\theta = \int_0^R g_r(r)\,dr\,,$$

where $R = 5$ is the maximum radius along the line of sight.

The lensing centroid x_κ is obtained by applying the rotation field $\phi(x, y)$ to the source profile; the dynamical centroid $x_{\rm dyn}$ is computed with the integrable part of the connection ($F = 0$). Their difference defines the centroid separation $\Delta x = x_\kappa - x_{\rm dyn}$.

9.4 Observational estimates

Order-of-magnitude estimate. Consider a galaxy lens at redshift $z_l \sim 0.5$ with mass $M \sim 10^{12} M_\odot$ and a distant source at $z_s \sim 1.0$. The Einstein radius is $R_E \sim 10\,\text{kpc} \sim 5\,\text{arcsec}$. In the pre-metric framework, the Faraday obstruction $F = dg$ is the curvature of the SO(2) connection, acting analogously to a magnetic field in the AB effect: it produces holonomy when integrated over a surface, even if $F = 0$ locally along the path. For a simple model where the connection is sourced by the lens's angular momentum or by a non-umbilic tidal field, we estimate the rotation angle over a typical line of sight as

$$\Delta\theta \sim \oint g \sim \int F\,dA \sim \kappa\,\frac{GM}{c^2 R_E}\,,$$

where κ is a dimensionless constant depending on the lens's internal structure. For a Schwarzschild lens, the optical index $n = (1-2M/r)^{-1/2}$ gives $g \approx (M/r)\,d\theta$ (at leading order). The integrated rotation along a ray passing at impact parameter $b \sim R_E$ is

$$\Delta\theta \sim \frac{GM}{c^2 R_E} \sim 10^{-5}\,\text{rad} \sim 2\,\text{mas}\,.$$

Thus we expect centroid shifts of the order of milliarcseconds (mas) for galaxy-scale lenses. For a cluster lens ($M \sim 10^{15}\,M_\odot$), the shift could reach $\sim 10\,\text{mas}$.

Noise and detectability. Current optical interferometers (VLTI, CHARA) achieve astrometric precision of $\sim 0.01\,\text{mas}$ for bright targets. The Gaia mission delivers parallaxes and proper motions at $\sim 0.02\,\text{mas}$ for $G \lesssim 15$. The forthcoming next-generation Very Large Array (ngVLA) and the Square Kilometre Array (SKA) will achieve microarcsecond precision in the radio band. Therefore, a centroid shift of $1-10\,\text{mas}$ is within reach of existing and near-future facilities, provided the signal can be distinguished from other astrometric perturbations (e.g., intrinsic source structure, microlensing).

Distinguishing from noise. The predicted centroid offset is single-signed for a given direction of the Faraday flux (sign of $\tilde{\rho}_0$). In contrast, random astrometric noise (e.g., from atmospheric turbulence, photon noise, or intrinsic source variability) averages to zero over many independent lines of sight or over time. The monotonic dependence on the twist amplitude

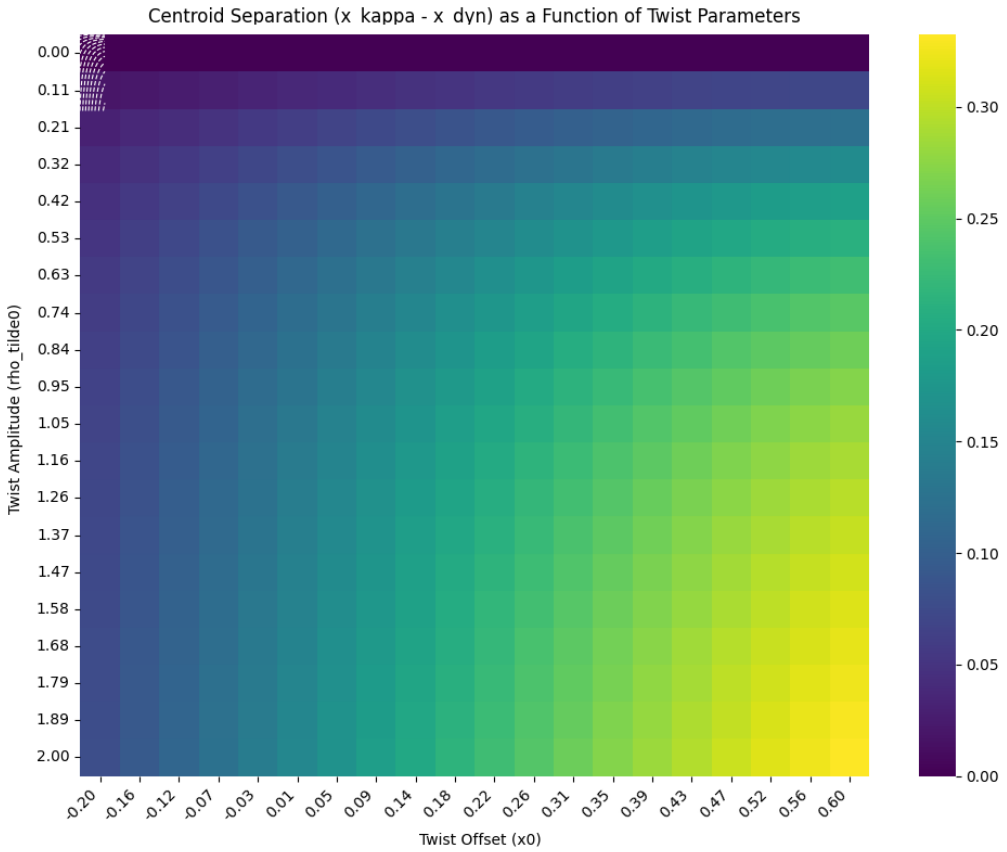

Fig. 2: Centroid separation $\Delta x(x_0, \tilde{\rho}_0)$ computed with the radial Lorentzian connection. The map is smooth, monotone, and strictly positive for $\tilde{\rho}_0 > 0$.

$\tilde{\rho}_0$ and offset x_0 provides a characteristic signature that can be searched for by stacking many lensed images. A detection of a systematic, non-zero mean centroid offset correlated with lens orientation would be a smoking gun for the pre-metric spin-1 sector.

10 Interferometric diagnostics: Michelson vs. Sagnac

Both Michelson and Sagnac interferometers (cf. Fig. 3) measure the relative phase difference between two paths. The difference lies in the **geometry of the paths**. A Michelson interferometer measures path-length differences between two reciprocal paths (out and back along the same arms). This measurement is sensitive to metric (spin-2) strains but not to the non-reciprocal holonomy of an SO(2) connection. The circulation of the connection cancels out because the paths are traversed in both directions.

A Sagnac interferometer sends beams in opposite directions around a closed loop. The phase difference is:

$$\Delta\theta = \frac{4\pi}{\lambda} \oint g = \frac{4\pi}{\lambda} \int F,$$

which is exactly the holonomy of the pre-metric connection. Thus, the Sagnac effect is the optical analogue of the AB effect: both measure the holonomy of a connection around a closed loop.

Therefore, to detect the spin-1 sector, one must use non-reciprocal loop-based measurements such as the Sagnac interferometer. The Michelson interferometer, by contrast, probes the metric shadow: both spin-0 and spin-2 sectors.

In other words, a Michelson interferometer measures the difference in optical path length between two arms. This is sensitive to:

- Spin-0 (scalar): Changes in the refractive index (or gravitational potential) that affect both arms equally or differently.
- Spin-2 (tensor): Metric strain (gravitational waves) that stretches one arm and compresses the other.

11 Information loss in physics: Dirac/Klein-Gordon and Hamiltonian/Lagrangian

The pre-metric/metric framework exhibits a pattern of information loss that appears repeatedly in theoretical physics.

11.1 Dirac/Klein-Gordon analogy

The Dirac equation describes a spin-1/2 fermion; its square (the Klein-Gordon equation) describes a spin-0 boson. One

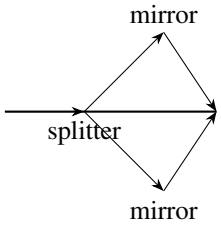

Michelson path-length difference

(a) Reciprocal (Michelson)

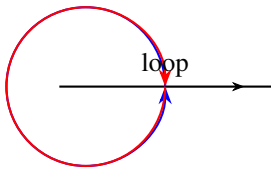

Sagnac
holonomy
$\Delta\phi \propto \oint g$

(b) Non-reciprocal (Sagnac)

Fig. 3: Comparison of reciprocal (Michelson) and non-reciprocal (Sagnac) interferometry. A Sagnac loop (at the bottom) measures holonomy (spin-1), whereas a Michelson interferometer (at the top) measures metric strain (spin-2).

cannot recover the Dirac spinor from the Klein-Gordon field because squaring loses fermionic information.

Similarly to this, squaring the pre-metric SO(2) connection $(g \wedge d\theta)^2$ produces a symmetric metric that contains only spin-0 and spin-2 components; the original spin-1 information (the connection g and its curvature $F = dg$) is irretrievably lost.

Thus the metric can be seen as a composite, coarse-grained object that discards spin-1 holonomy. This analogy supports the view that the pre-metric connection is geometrically more fundamental, while the metric is its spin-2 shadow.

11.2 Hamiltonian/Lagrangian analogy

There is a deeper structural analogy between the pre-metric/metric framework and the Hamiltonian/Lagrangian formulations of classical mechanics.

In Hamiltonian mechanics, the primary object is the Hamiltonian $H(q, p)$, from which the Lagrangian $L(q, \dot{q})$ is obtained via the Legendre transform:

$$L = p\dot{q} - H\,.$$

The constant of integration in this transform is the total energy E, which is not explicitly visible in the Lagrangian formulation. The Hamiltonian contains both position and momentum information; the Lagrangian loses the independent momentum degree of freedom.

Similarly, in our pre-metric framework, the connection g is the primary geometric object. The metric is obtained via the quadratic embedding:

$$(d\theta + g)^2.$$

The constant of integration in this embedding is the harmonic component ω_{harm} (topological monodromy), which is not visible in the metric. The connection contains spin-0, spin-1, and spin-2 information; the metric loses the spin-1 (connection) information.

This analogy reinforces the view that the pre-metric connection is the more fundamental geometric object, while the metric is a derived, coarse-grained object that discards spin-1 holonomy — just as the Lagrangian discards the total energy when obtained from the Hamiltonian.

12 Fictitious vs. real forces in gravity

The equivalence principle asserts that the connection coefficients (Christoffel symbols) can be made to vanish at a point by a suitable choice of coordinates (free fall). In the pre-metric language, this corresponds to the possibility of locally eliminating the spin-1 connection g when it is a pure gradient. However, the curvature $F = dg$ (spin-0) and the quadratic tidal term $(g_t - g_r)^2$ (spin-2) are coordinate-invariant obstructions that cannot be removed. For a static observer in Schwarzschild geometry, the fictitious acceleration is M/r^2 (proportional to Γ^r_{tt}), while two nearby observers measure the tidal acceleration M/r^3 (proportional to R^r_{trt}). The latter is observer-independent and constitutes the genuine gravitational field.

12.1 Why metric theories and MOND cannot produce the spin-1 centroid effect

GR is a metric theory: the fundamental field is the metric $g_{\mu\nu}$, and the Levi-Civita connection is derived from it. TeVeS (Bekenstein 2004 [14]) introduces additional fields (a vector and a scalar) but does not modify the Einstein equations; it adds terms to the action. The gravitational sector still uses the metric and its Levi-Civita connection. Consequently, in the language of the pre-metric decomposition, the angular connection is integrable: $F = dg = 0$. The only possible parallel transport effect on the angular fibre would be monodromy from non-contractible loops (topological), not a local curvature-driven rotation.

MOND (Milgrom 1983 [15]) is not a metric theory; it is a phenomenological modification of Newtonian dynamics, replacing the acceleration law $a = GM/r^2$ by $a = \sqrt{GMa_0}\,/r$ in the deep-MOND regime. Relativistic extensions (such as TeVeS) attempt to embed MOND into a metric framework, but they still rely on a metric-compatible connection, so $F = 0$ holds. In the pre-metric framework, the integrable $(F = 0)$ sector corresponds to a scalar potential $\Phi = \ln G$; this

Hamiltonian Formulation	Pre-metric Framework
Primary object: Hamiltonian $H(q, p)$	Primary object: Connection g
Secondary object: Lagrangian $L(q, \dot{q})$	Secondary object: Metric $(d\theta + g)^2$
Loses: Independent momentum $\dot{q}$	Loses: Spin-1 (connection)
Constant of integration: Total energy E	Constant of integration: Monodromy ω_{harm}
Dynamics: Hamilton's equations	Dynamics: Connection action

Table 3: Spin decomposition of the SO(2) connection on a 2-D basis.

includes the MOND limit as a special case (§8.4) but cannot generate the spin-1 centroid separation.

Thus, all metric theories (GR, TeVeS) and the original MOND have $F = 0$ in the present language. The centroid separation predicted in this paper arises from a non-integrable connection ($F \neq 0$), which is a purely spin-1 geometric effect. A detection of the predicted single-signed centroid offset would therefore rule out all metric theories of gravity and their MOND extensions, providing a sharp observational test.

13 Curvature decomposition, Weyl tensor, and spin channels in metric gravity vs. pre-metric framework

In standard (pseudo-)Riemannian geometry, the connection 1-form ω^a_b (Levi-Civita) and its curvature 2-form

$$R^a_b = d\omega^a_b + \omega^a_c \wedge \omega^c_b$$

contain the full gravitational field. The decomposition of R^a_b into irreducible representations of the Lorentz group yields:

- Spin-0: the trace of the Ricci tensor, i.e., the Ricci scalar $R = g^{ab}R_{ab}$.
- Spin-1: the antisymmetric part of the Ricci tensor (vanishes in GR because $R_{[ab]} = 0$ due to the first Bianchi identity; for a non-metric connection this could appear)
- Spin-2: the traceless part of the Ricci tensor (the Ricci tensor minus its trace) and the Weyl tensor C_{abcd}, which is completely traceless and represents the radiative degrees of freedom of gravity.

The quadratic term $\omega \wedge \omega$ is the source of the non-linearity of gravity and gives rise to the Weyl tensor. In fact, if one attempts to linearise the curvature, the $\omega \wedge \omega$ term is of second order and is discarded, leading to the linearised wave equation for metric perturbations. The full non-linear theory retains this term, which is essential for gravitational wave emission, black hole formation, and the self-interaction of gravity.

13.1 Equivalence principle and the elimination of the connection

The equivalence principle states that at any point one can choose coordinates (geodesic coordinates) such that $\omega^a_b = 0$ at that point. However, the curvature R^a_b involves both first derivatives of ω (the $d\omega$ term) and products of ω (the $\omega \wedge \omega$ term). Even after setting $\omega = 0$ at a point, the derivatives of ω and the products of ω at neighbouring points remain, so the curvature cannot be made zero. This is why the equivalence principle eliminates the fictitious "force" (the connection) but not the genuine "field" (the curvature).

13.2 The Weyl tensor, Ricci tensor, and gravitational radiation

The Riemann tensor admits the algebraic decomposition

$$R_{abcd} = C_{abcd} + \frac{1}{2}\left(g_{ac}R_{bd} - g_{ad}R_{bc} - g_{bc}R_{ad} + g_{bd}R_{ac}\right) - \\ - \frac{R}{6}\left(g_{ac}g_{bd} - g_{ad}g_{bc}\right),$$

where C_{abcd} is the Weyl tensor (trace-free), and the remaining terms are constructed from the Ricci tensor R_{ab} and Ricci scalar R.

It is a common misconception that only the Weyl tensor carries gravitational radiation. This is only true in vacuum GR ($R_{ab} = 0$), where the Riemann tensor equals the Weyl tensor. In general, the Ricci tensor can also carry propagating degrees of freedom:

- **Spin-0 (scalar) radiation**: In scalar-tensor theories (e.g., Brans-Dicke, $f(R)$ gravity), the Ricci scalar R carries scalar gravitational waves.
- **Spin-1 (vector) radiation**: In theories with torsion or non-metricity, the antisymmetric part of the Ricci tensor can propagate.
- **Spin-2 (tensor) radiation**: Both the Weyl tensor and the traceless part of the Ricci tensor can contribute to tensor modes.

Thus, every spin component of the curvature can have radiative modes. The Weyl tensor is not the sole carrier of gravitational radiation; it is simply the trace-free part of the Riemann tensor that dominates in vacuum GR.

In the pre-metric SO(2) framework, the curvature is simply $F = dg$ (a scalar 2-form), which carries spin-0 radiation. The spin-2 tidal term $(g_t - g_r)^2$ is not a curvature but an algebraic quadratic invariant. There is no analogue of the Weyl tensor; the spin-2 effect is purely algebraic, not radiative, in the Abelian phase. However, when the framework is extended to the non-Abelian SO(3) regime, additional radiative modes may appear.

13.3 Contrast with the pre-metric SO(2) framework

In the pre-metric SO(2) framework presented in this paper:

The connection is Abelian: $g = g_a\,dx^a$ (a single 1-form). Its curvature is $F = dg$ with no $\omega \wedge \omega$ term because the Lie algebra is 1-dimensional and the wedge product of two 1-forms is symmetric, hence vanishes. The spin-0 channel is the curvature F (a scalar in 2D). This is an obstruction to integrability: when $F \neq 0$, the connection is non-integrable and produces holonomy. The spin-1 channel is the connection g itself (a vector in 2D). Its components define the twist and carry spin-1 information that is erased by the quadratic embedding. The spin-2 tidal term $(g_t - g_r)^2$ arises from the quadratic embedding of the connection into a metric, not from curvature. It is an algebraic quadratic invariant of the connection, representing the deviation from umbilicity.

There is no analogue of the Weyl tensor in the pre-metric SO(2) framework because the curvature is simply $F = dg$ — a scalar 2-form. The spin-2 effect is algebraic, not curvature-derived, in the Abelian phase. However, this does not imply that spin-2 is inherently non-radiative. Rather, it reflects the fact that in the SO(2) regime, the spin-2 effect arises from the embedding, not from curvature. When the framework is extended to the non-Abelian SO(3) regime, the failure of the normality condition introduces additional curvature components (the $\omega \wedge \omega$ terms), which may carry radiative modes — including spin-2 radiation.

Thus, while GR conflates spin-0 and spin-2 in the full Riemann curvature (and then separates them via the Weyl decomposition), the pre-metric framework keeps these channels distinct from the outset. The spin-1 Faraday sector is linear in the SO(2) regime; the non-linear terms appear only when we transition to the non-Abelian SO(3) regime, where additional curvature obstructions arise from the embedding geometry. These terms are 'sources' of curvature, rather than being curvature themselves.

13.4 Conclusion

In standard (pseudo-)Riemannian geometry, the curvature 2-form

$$R^a_b = d\omega^a_b + \omega^a_c \wedge \omega^c_b$$

contains both the derivative term $d\omega$ and the quadratic commutator term $\omega \wedge \omega$. The algebraic decomposition of R^a_b into Weyl and Ricci parts separates the trace-free (Weyl) and Ricci contributions. However, this algebraic decomposition does *not* imply that only the Weyl tensor radiates. In general, the Ricci tensor and Ricci scalar can also carry propagating degrees of freedom, depending on the theory and the presence of matter.

In the pre-metric SO(2) framework, the curvature is simply $F = dg$ with no $\omega \wedge \omega$ term because the Lie algebra $\mathfrak{so}(2)$ is 1-dimensional. This does not mean that the SO(2) framework is weak or incomplete — it already contains genuine curvature (holonomy) and produces observable spin-1 effects (centroid separation) that are completely absent in metric theories.

The quadratic term $\omega \wedge \omega$ appears only when the fibre thickens from S^1 to S^2 (the non-Abelian SO(3) regime). In that case, the 2D leaves need to be oriented into higher dimensions; the $\omega \wedge \omega$ terms act as sources of additional curvature contributions for the non-Abelian structure, analogous to the Γ^2 terms in the Riemann tensor. These terms are not the source of gravity itself — gravity already exists in the SO(2) framework via $F = dg$. Rather, they are contributions that arise when the geometry is embedded in higher dimensions.

Thus, while the algebraic decomposition of the Riemann curvature in GR separates spin-0 and spin-2 contributions, the pre-metric framework keeps these channels distinct from the outset. The spin-1 Faraday sector is linear in the SO(2) regime; the non-linear terms appear only when we transition to the non-Abelian SO(3) regime.

14 How far can we go with the connection in describing gravity?

The pre-metric SO(2) connection g captures a genuine spin-1 geometric degree of freedom that is completely erased when one passes to a symmetric metric via the quadratic embedding $(d\theta+g)^2$. This raises the question: what aspects of gravity can be described using only the connection, and where does the metric become indispensable?

What the connection alone can describe

- **Holonomy and monodromy**: Parallel transport of vectors on the fibre is governed solely by g. The curvature $F = dg$ gives local holonomy, while the harmonic part of g encodes topological monodromy (AB type). Both are independent of any base metric.
- **Spin-1 lensing signature**: A non-integrable connection ($F \neq 0$) produces a centroid separation in gravitational lensing. This effect is purely connection-driven and cannot be mimicked by metric shear or flexion.
- **Optical interpretation**: The Gauss-Log-Index projection principle derives g directly from a refractive index $n(r)$ without invoking a metric on the base. The connection then determines the bending of light via the Cartan structure equations.

What requires the metric

- **Distance and time measurements**: A metric is needed to define proper distances, light travel times, and the causal structure of spacetime. The connection alone does not provide a notion of length or interval.
- **Coupling to matter**: Matter can be introduced via cyclic coordinates in the total metric that require mechanical conservation like energy and angular momentum.

15 Conclusions

We have developed a pre-metric SO(2) connection framework that cleanly separates the spin-0, spin-1, and spin-2 channels of an angular bundle over a two-dimensional base. The Hodge decomposition identifies a topological monodromy (real AB rotation) independent of local curvature. The quadratic embedding $(d\theta + A)^2$ (with θ denoting the generic fibre coordinate, which is θ in our S^1 case) is proved non-invertible: the antisymmetric curvature dA (spin-1) is erased by symmetrization and cannot be recovered from the symmetric metric block.

When the normality condition of a fibre embedding fails, the structure group enlarges from SO(2) to SO(3), and the curvature acquires quadratic commutator terms of Yang-Mills type, providing a geometric origin for non-Abelian self-interaction.

The spin-1 Faraday sector, characterised by $F = dg \neq 0$, produces observable SO(2) holonomy in gravitational lensing, manifest as a centroid separation between lensing and dynamical channels. Numerical illustrations on a uniform $(x_0, \tilde{\rho}_0)$ grid yield a smooth, monotone, single-signed heatmap that demonstrates the predicted coupling. This signature is absent in all metric theories (GR, MOND, TeVeS) because they impose $F = 0$ [14–16].

We have shown that the AB effect is a classical optical holonomy — a spin-1 geometric phenomenon that is neither electrodynamic nor quantum in origin. It provides the fundamental experimental validation of the pre-metric framework, demonstrating that connection holonomy has observable physical consequences independent of any metric. This geometric interpretation unifies gravitational lensing and the AB effect as manifestations of the same underlying principle: the physical reality of the connection.

This refutes the anyon postulate (Wilczek, 1982 [4, 5]), which misinterprets the AB effect as a quantum statistical phenomenon. As shown in Lavenda and Dunning-Davies (1989 [6]), no probability distribution exists between the binomial (fermionic) and negative binomial (bosonic) distributions, rendering intermediate statistics stillborn. The AB effect demonstrates spin-1 holonomy; it says nothing about fermionic exchange statistics.

Appendix

Numerical protocol

The centroid separation $\Delta x(x_0, p)$ is computed by integrating the transport equation along a radial line of sight. The following pseudo-code outlines the algorithm:

```
for each x0 in grid:
  for each p in grid:
    define radial connection with Lorentzian profile (a = 1)
    define g_r(r) = - p * (r - x0) / ((r - x0)^2 + 1)
    w = 1 + 0i   # initial image basis
    for r from 0 to 5 step 0.001:   # R = 5, dr/dlambda = 1
        Omega = g_r(r)
        w = RK4_step(w, Omega, dr)   # fourth-order Runge-Kutta
    phi_lens = arg(w)   # final rotation angle
    # reference: integrable part (p = 0) gives zero rotation
    Delta_x[x0, p] = phi_lens
```

Received on June 11, 2026

References

1. Hodge W. V. D. The Theory and Applications of Harmonic Integrals. Cambridge University Press, 1941.
2. Kobayashi S. and Nomizu K. Foundations of Differential Geometry, Vol. I. Wiley, 1963.
3. Bleecker D. Gauge Theory and Variational Principles. Dover, 2005.
4. Wilczek F. Magnetic flux, angular momentum, and statistics. *Phys. Rev. Lett.*, 1982, v. 48, 1144.
5. Wilczek F. Quantum mechanics of fractional-spin particles. *Phys. Rev. Lett.*, 1982, v. 49, 957.
6. Lavenda B. H. and Dunning-Davies J. The case against intermediate statistics. *J. Math. Phys.*, 1989, v. 30 (5), 1117–1121.
7. Nakahara M. Geometry, Topology and Physics. Taylor & Francis, 2003.
8. Arnowitt R., Deser S. and Misner C. W. In "Gravitation": An Introduction to Current Research. Wiley, 1962.
9. Appelquist T., Chodos A. and Freund P. G. O. (eds.). Modern Kaluza-Klein Theories. Addison-Wesley, 1987.
10. do Carmo M. P. Riemannian Geometry. Birkhäuser, 1992.
11. Spivak M. A Comprehensive Introduction to Differential Geometry, Vol. II. Publish or Perish, 1979.
12. Lavenda B. Seeing Gravity. 2nd ed. Self-published, 2024, §2.2.
13. Luneburg R. K. Mathematical Theory of Optics. University of California Press, 1964, §29.
14. Bekenstein J. D. Relativistic gravitation theory for the modified Newtonian dynamics paradigm. *Phys. Rev. D*, 2004, v 70, 083509.
15. Milgrom M. A modification of the Newtonian dynamics as a possible alternative to the hidden mass hypothesis. *Astrophys. J.*, 1983, v. 270, 365.
16. Einstein A. Die Grundlage der allgemeinen Relativitätstheorie. *Ann. Phys.*, 1916, v. 49, 769.
17. Frankel T. The Geometry of Physics. Cambridge University Press, 2011.
18. Baez J. and Muniain J. P. Gauge Fields, Knots and Gravity. World Scientific, 1994.